Steric interaction between spherical colloidal particles

Aileen Lozsán,* Máximo García-Sucre,† and German Urbina-Villalba‡
Centro de Física, Instituto Venezolano de Investigaciones Científicas (IVIC), Caracas 21827, Venezuela
(Received 20 June 2005; published 22 December 2005)

The reliability of the Derjaguin approximation for the calculation of the mixing term between sterically stabilized colloidal particles is studied. For this purpose, the steric potential obtained from the experiment of Doroszkowski and Lambourne [J. Polym. Sci., Part C: Polym. Symp. **34**, 253 (1971)] is regarded as an exact result. Several analytical expressions corresponding to the mixing term of the steric potential are tested. Vincent *et al.* [Colloids Surf. **18**, 261 (1986)] obtained four of them using the Derjaguin approximation along with different profiles for the volume fraction of segments in grafted polymer layers. As will be shown, the exact calculation of the volume of interaction between two spheres with adsorbed polymer layers already leads to a considerable improvement of the theoretical prediction for the simplest case of constant spatial distribution of polymer monomers. This equation is also better than the four additional expressions that result from using Bagchi's formalism [J. Colloid Interface Sci. **47**, 86 (1974)] with similar segment profiles. The deviations of Bagchi's formalism can be substantially minimized using Flory-Krigbaum theory instead of the Flory-Huggins formalism for the calculation of the free energy of mixing. The equations derived here for the steric potentials were derived for particles of distinct radii.

DOI: 10.1103/PhysRevE.72.061405 PACS number(s): 82.70.Dd, 82.70.Kj, 83.10.Mj, 47.55.Dz

I. INTRODUCTION

The prediction of the steric interaction between two spheres covered by grafted polymers has been a subject of study since the 1950s [1–11]. Earlier approaches divided the calculation of the steric potential into two steps [3,5–7]. The first one concerned the calculation of the spatial distribution of polymer segments in the vicinity of a planar surface. The second one dealt with the actual evaluation of the free energy employing theoretical distribution functions of polymer segments [3,5–7]. Except for very few cases [2] the expressions of the free energy were initially deduced for two planar surfaces, and required the use of the Derjaguin approximation [12] in order to obtain the potential of interaction between two spherical particles.

The behavior of polymers attached to a planar surface has been successfully described by several theories, in particular by the single chain mean field theory of Szleifer [13] and the self-consistent approach of Scheutjen and Fleer [14]. The scaling theory of de Gennes [15] was validated satisfactorily by Tauton *et al.* [16] using the surface force apparatus (SFA). Unfortunately, there is no unified theory for the treatment of the steric stabilization between suspended particles. This situation result from the marked differences between the distributions of polymer segments attached to either planar surfaces or spherical particles.

The complexity of the first step referred to above can be avoided by implementing simple mathematical models that resemble the experimental behavior of polymers near a flat surface [1,2,4,8–11]. In this respect, Vincent *et al.* [1] suggested four simple expressions for the distribution of monomers that can be exactly integrated following the Derjaguin approximation. Thus, these equations are commonly used in simulations of sterically stabilized particles [17–19]. Their model is based on the earlier ideas of Smitham *et al.* [11] and Meier [5] in which the steric interaction is visualized as the consequence of two stabilizing contributions. The first one has an osmotic origin and is caused by the interpenetration of the adsorbed polymer chains corresponding to each interacting surface. These chains "mix" in the region of overlap, generating a high density of polymer. Depending on the affinity between the polymer and the solvent, the solvent molecules can migrate toward or away from the region of overlap. In the case of a good solvent, the high concentration of polymer generates a flux of solvent molecules toward the overlapping region causing the separation of the interacting particles. This effect occurs during the whole range of the steric interaction which begins at interparticle distances (h) lower than twice the width of the adsorbed polymer layers (2δ). The second contribution, usually referred as "elastic," also has an entropic origin. It results from the elastic compression of the adsorbed chains. This limitation of the available volume leads to a loss in the configurational entropy of the chains, which is most significant when $h < \delta$.

Recently, Oversteegen and Lekkerkerker [20] outlined the importance of the exact calculation of the volume of overlap for the depletion potential between large spheres in the presence of small spheres, disks, or rods. Since the depletion potential results from the exclusion of the small particles from the overlap region, the exact evaluation of this volume determines the number of small particles that can be excluded. Consequently, the exactness of the theoretical potential and the phase behavior of the large particles can be erroneously approximated due to the underestimation of the exact solution because of the neglected curvature. In the case of the steric interaction, the repulsive force depends on the amount of polymer segments that can be accommodated in-

*Corresponding author. Electronic address: alozsan@ivic.ve
†Electronic address: mgs@ivic.ve
‡Electronic address: guv@ivic.ve

side the overlap region. Since that quantity is already known to vary significantly with the spatial distribution of segments, it is expected that the accuracy of the steric potential might be improved, avoiding the implementation of the Derjaguin approximation. The results of this investigation support this hypothesis.

In this paper we first use the expression of Vincent *et al.* [1] for the mixing energy in order to approximate the mixing interaction between two spheres of different radii stabilized by adsorbed polymer layers. The interaction potential was evaluated using the exact volume of the region of overlap analytically calculated in this work. Since the integrals required are difficult to compute, the polymer layer was characterized by a fixed width (δ) and a uniform distribution of polymer segments ($\bar{\phi}_2$). This model will be further referred to as the extended Vincent (EV) model. Additionally, we have implemented the four analytic distributions of polymers suggested by Vincent *et al.* [1] in the formalism of Bagchi [2], which computes the volume of overlap, avoiding the use of the Derjaguin approximation. For this purpose, the dependence of the mentioned distributions on the distance of approach between two planar surfaces was substituted by the radial separation between the spherical particles. This second model will be referred as the extended Bagchi (EB) model.

In order to test the accuracy of the theoretical predictions, we use here the steric potential measured by Doroszkowski and Lambourne [9,21]. Although several experiments have evaluated the steric interaction between two planar surfaces [22–24], only a few studies deal with the case of spherical particles. Indirect approximations of the steric potential between spheres are available [25]. However, up to our knowledge there are only two experiments that directly determine the steric interaction force between two suspended particles. Doroszkowski and Lambourne [9,21] used a Langmuir trough in order to measure the variation of the surface pressure as a function of the available surface area for spheres of polyacrylonitrile at a toluene/water interface. This allowed them to compute the work done for compressing the polymer layers of the particles. More recently, Leal-Calderon and coworkers [26,27] used a magnetic field over drops of a ferrofluid in order to measure the steric potential. Under specific experimental conditions the drops of this fluid can be aligned in a chainlike formation and its potential calculated. Unfortunately, the resulting empirical equation is a function of a few effective variables, and does not show an explicit analytical dependence on several relevant parameters of the steric potential.

II. GENERAL EXPRESSION FOR THE FREE ENERGY OF MIXING

Consider two surfaces k and l either flat or curved [Fig. 1(a)], each one covered with a polymer layer of width δ, initially separated by a very long distance ($h=\infty$). The polymer layers are already in contact with the solvent medium. However, their entropy changes significantly when they are brought together until they overlap [Fig. 1(b)], or even closer, up to the distance where the elastic compression of the chains begins [Fig. 1(c)]. Let us call $\Delta G_S(h)$ the change

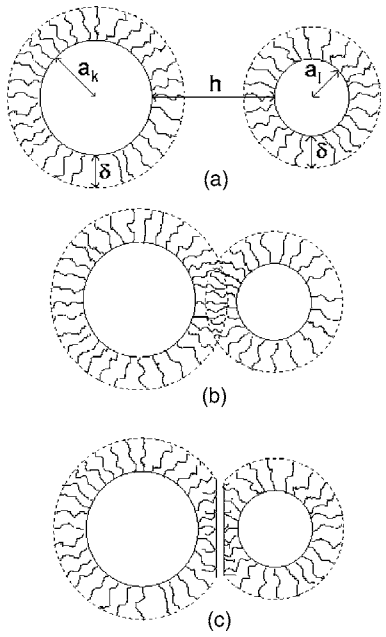

FIG. 1. Steric interaction between two spherical particles covered by polymer layers. (a) $h=\infty$, (b) $\delta<h<2\delta$, and (c) $0<h<\delta$.

in the free energy of the complete process of bringing together the spheres from infinity to a distance h. This thermodynamic potential is usually considered to be the sum of two contributions:

$$\Delta G_S(h) = \Delta G_M + \Delta G_{el}. \tag{1}$$

The first term on the right hand side, ΔG_M, corresponds to the change in the free energy of mixing of polymer segments and solvent molecules. It has a nonzero value for distances lower than 2δ ($h<2\delta$). The second term ΔG_{el} (elastic), accounts for the decrease of the configurational free energy of the polymer molecules due to the reduction of the available volume as a consequence of the approach of the opposite surface. It takes significant values for distances of the order of δ ($h<\delta$).

According to Vincent *et al.* [1], ΔG_M can be calculated using the well-known method employed by Flory and Krigbaum [28,29] to evaluate the change in the free energy of mixing when two polymer molecules of surfaces k and l are brought together in volume dV, starting from an infinite distance of separation. The general expression obtained for this term is

$$\Delta G_M(h) = \frac{k_B T V_s^2}{V_1}\left(\frac{1}{2}-\chi\right)(A\Gamma_\nu)^2\left(\int_V (\hat{\rho}_k^2 + 2\hat{\rho}_k\hat{\rho}_l + \hat{\rho}_l^2)_h dV - \int_V \hat{\rho}_{k,\infty}^2 dV - \int_V \hat{\rho}_{l,\infty}^2 dV\right), \quad 0<h<2\delta. \tag{2}$$

Here k_B is the Boltzmann constant, T the absolute temperature, V_s the volume of a polymer segment, V_1 the volume of a molecule of solvent, χ the interaction parameter of Flory-Huggins, A the surface area of each interacting body, Γ_ν the number of segments per unit area, and $\hat{\rho}_k$ and $\hat{\rho}_l$ the normalized distribution functions of polymer over surfaces k and l,

respectively. Subscripts ∞ and h refer to the distance of separation between the surfaces.

However, it can be supposed that in the region $\delta < h < 2\delta$, the chains of polymer coming from the two surfaces only interpenetrate each other [1]. In this case the initial distribution of polymer does not change appreciably in the overlap region, and the amount of solvent molecules adjusts itself to the final available volume. That is, $\hat{\rho}_{k,\infty} = \hat{\rho}_{k,h}$ and $\hat{\rho}_{l,\infty} = \hat{\rho}_{l,h}$. In this case, Eq. (2) can be simplified, yielding

$$\Delta G_M(h) = \frac{2k_B T V_s^2}{V_1}\left(\frac{1}{2} - \chi\right)(A\Gamma_\nu)^2 \int_V (\hat{\rho}_k \hat{\rho}_l)_\infty dV, \qquad (3)$$

$$\delta < h < 2\delta.$$

In Eqs. (2) and (3), the integration is carried out over the volume of overlap which is determined by the geometry of the interacting bodies.

In the region $0 < h < \delta$, compression of the chains unavoidably occurs along with the interpenetration of the polymer molecules. In this case, the previous assumptions are not valid and Eq. (2) must be evaluated.

Solving the integrals of Eqs. (2) and (3) for the case of two planar surfaces covered by polymer layers, the free energy of interaction per unit area between flat plates (superscript *fp*) results $[\Delta^{fp} G_M(d)]$. As usual, this can be related to the free energy of interaction between two different spherical particles by means of the Derjaguin approximation:

$$\Delta^S G_M(h) = 2\pi \frac{a_k a_l}{a_k + a_l} \int_h^{2\delta} \Delta^{fp} G_M(d) dd, \quad h, \delta \ll a. \qquad (4)$$

In Eq. (4), $\Delta^S G_M(h)$ is the energy of steric interaction between two spherical particles of radii a_k and a_l, d is the distance of approach between the planar surfaces, and h is the closest approach between the spherical particles.

The approximation above was initially applied for the computation of forces that do not involve any volume of overlap between the interacting bodies. Examples of these are electrostatic and van der Waals forces. Unlike these forces, the steric interaction is zero until the overlap of the interacting polymer layers occurs. Equation (4) results from the calculation of the energy of interaction between circular rings defined at the surface of each sphere. These rings are supposed to be flat surfaces. Hence, the polymer molecules are implicitly assumed to be perpendicular to each ring, as occurs in the case of two flat surfaces. However, it is clear that the polymer molecules are oriented in the radial direction when they are attached to a spherical particle. As a result, the polymer density calculated in the region of overlap is overestimated (see below).

III. EV MODEL

This model was developed in this work to avoid the use of the Derjaguin approximation. With this objective, we solved the integrals of Eq. (2) explicitly evaluating them over the overlap volumes indicated in Figs. 2(a) and 2(b).

In the case of two spherical particles of radius a_k and a_l, and surfaces areas A_k and A_l, the steric potential in the region $\delta < h < 2\delta$ [Fig. 2(a)] is equal to

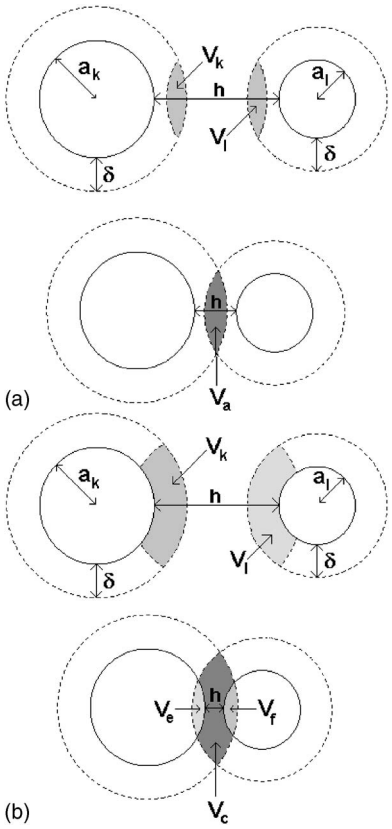

FIG. 2. Model for the calculation of the mixing potential in EV and EB models. (a) $\delta < h < 2\delta$, (b) $0 < h < \delta$.

$$\Delta G_M(h) = \frac{2k_B T}{V_1}\left(\frac{1}{2} - \chi\right)(A_k A_l)(\Gamma_\nu V_s)^2 \int_{V_a} (\hat{\rho}_k \hat{\rho}_l)_\infty dV, \qquad (5)$$

$$\delta < h < 2\delta,$$

where V_a is the effective volume of overlap between two spheres of different radii [Fig. 2(a)]. Identification of the region of interaction in terms of a convenient set of variables [Fig. 3(a)] leads to the establishment of the following limits for the integral appearing in Eq. (5):

$$\int_{V_a} (\hat{\rho}_k \hat{\rho}_l)_\infty dV = \int_0^{2\pi} \int_0^{\arccos(p/R_k)} \times \int_{H\cos(\varphi) - [R_l^2 + H^2\cos^2(\varphi) - H^2]^{1/2}}^{R_k} (\hat{\rho}_k \hat{\rho}_l)_\infty \varrho^2 \times \sin(\varphi) d\varrho \, d\varphi \, d\theta \qquad (6)$$

where the distance p is indicated in Fig. 3(a).

In the region $0 < h < \delta$ the equation to be solved is similar to Eq. (2), except for the fact that in this case, particles of different radii have to be considered:

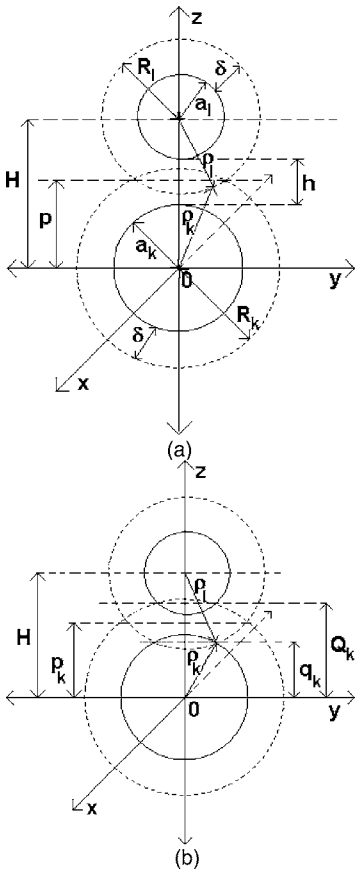

FIG. 3. Coordinate axes for the calculation of the mixing potential in EV and EB models. (a) $\delta < h < 2\delta$, (b) $0 < h < \delta$.

$$\Delta G_M(h) = \frac{k_B T}{V_1}\left(\frac{1}{2} - \chi\right)\left[(A_k\Gamma_\nu V_s)^2\left(\int_{V_c}\hat{\rho}_{k,h}^2 dV - \int_{V_k}\hat{\rho}_{k,\infty}^2 dV\right) + (A_l\Gamma_\nu V_s)^2\left(\int_{V_c}\hat{\rho}_{l,h}^2 dV - \int_{V_l}\hat{\rho}_{l,\infty}^2 dV\right)\right] + \frac{2k_B T}{V_1}\left(\frac{1}{2} - \chi\right)(A_k\Gamma_\nu V_s) \times (A_l\Gamma_\nu V_s)\int_{V_c}\hat{\rho}_{k,h}\hat{\rho}_{l,h} dV, \quad 0 < h < \delta. \tag{7}$$

In this last equation, the integrations should be carried out over the volumes V_k, V_l, and V_c which can be defined by identifying the overlap volumes on each sphere before and after the actual overlap occurs [see Fig. 2(b)]:

$$\int_{V_k} dV = \int_0^{2\pi}\int_0^{\arccos(p_k/R_k)}\int_{H\cos(\varphi)-[R_l^2 + H^2\cos^2(\varphi) - H^2]^{1/2}}^{R_k} \varrho^2 \times \sin(\varphi) d\varrho\, d\varphi\, d\theta - \int_0^{2\pi}\int_0^{\arccos(q_k/a_k)}\int_{H\cos(\varphi)-[R_l^2 + H^2\cos^2(\varphi) - H^2]^{1/2}}^{a_k} \varrho^2 \times \sin(\varphi) d\varrho\, d\varphi\, d\theta, \tag{8}$$

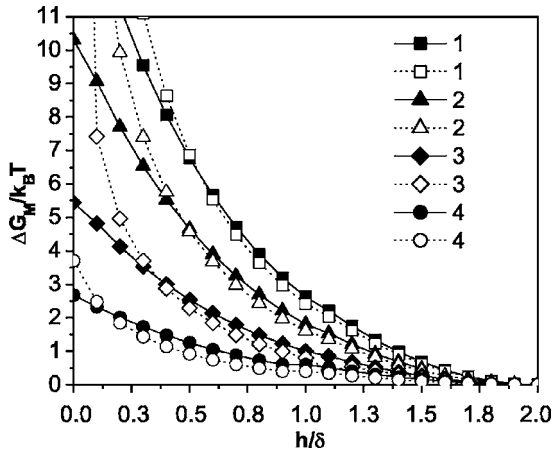

FIG. 4. Comparison between EV model (closed symbols) and the original Vincent model (open symbols) for different radii of particles ($a_k = a_l$, $\delta = 14.7$ nm): 1 = 150, 2 = 100, 3 = 50, and 4 = 25 nm.

$$\int_{V_l} dV = \int_0^{2\pi}\int_0^{\arccos(p_k/R_k)}\int_{H\cos(\varphi)-[R_l^2 + H^2\cos^2(\varphi) - H^2]^{1/2}}^{R_k} \varrho^2 \times \sin(\varphi) d\varrho\, d\varphi\, d\theta - \int_0^{2\pi}\int_0^{\arccos(Q_k/R_k)}\int_{H\cos(\varphi)-[a_l^2 + H^2\cos^2(\varphi) - H^2]^{1/2}}^{R_k} \varrho^2 \times \sin(\varphi) d\varrho\, d\varphi\, d\theta, \tag{9}$$

$$\int_{V_c} dV = \int_{V_k} dV - \int_0^{2\pi}\int_0^{\arccos(Q_k/R_k)}\int_{H\cos(\varphi)-[a_l^2 + H^2\cos^2(\varphi) - H^2]^{1/2}}^{R_k} \varrho^2 \times \sin(\varphi) d\varrho\, d\varphi\, d\theta \tag{10}$$

where distances p_k, q_k, and Q_k are shown in Fig. 3(b), and can be evaluated from the following relations (where $R_k = a_k + \delta$):

$$p_k = \frac{R_k^2 - R_l^2 + H^2}{2H}, \tag{11a}$$

$$q_k = \frac{a_k^2 - R_l^2 + H^2}{2H}, \tag{11b}$$

$$Q_k = \frac{R_k^2 - a_l^2 + H^2}{2H}. \tag{11c}$$

In order to obtain an analytic solution for $\Delta G_M(h)$, it is necessary to choose a simple form for the distribution functions $\hat{\rho}$. Due to the complexity of the integrals we selected a constant distribution function along the radial direction of the particles. Accordingly,

$$\phi_k(\varrho - a_k) = \bar{\phi}_{2,k}, \tag{12}$$

$$\phi_l(\varrho' - a_l) = \phi_l(\varrho'') = \bar{\phi}_{2,l}, \tag{13}$$

where $\bar{\phi}_{2,k}$ and $\bar{\phi}_{2,l}$ are the average volume fractions of polymers in each polymer layer. ϱ'' is the radial coordinate $\varrho' - a_l$ transformed in such a way that it can be located on the coordinate axis $\varrho - a_k$ which is fixed to the center of mass of particle k. In the case of a constant distribution of polymer segments, the transformation does not affect the functional form of the distribution because no explicit dependence of the radial coordinate exists. Functions $\hat{\rho}_k$ and $\hat{\rho}_l$ can be obtained from the above expressions, considering that, for the region $\delta < h < 2\delta$,

$$\bar{\phi}_{2,k} = \frac{\Gamma_\nu V_s A_k}{V_a}, \quad \hat{\rho}_{k,\infty} = \frac{1}{V_a}, \tag{14}$$

$$\bar{\phi}_{2,l} = \frac{\Gamma_\nu V_s A_l}{V_a}, \quad \hat{\rho}_{l,\infty} = \frac{1}{V_a}, \tag{15}$$

and, for the region $0 < h < \delta$,

$$\bar{\phi}_{2,k} = \frac{\Gamma_\nu V_s A_k}{V_k}, \quad \hat{\rho}_{k,h} = \frac{1}{V_c}, \quad \hat{\rho}_{k,\infty} = \frac{1}{V_k}, \tag{16}$$

$$\bar{\phi}_{2,l} = \frac{\Gamma_\nu V_s A_l}{V_l}, \quad \hat{\rho}_{l,h} = \frac{1}{V_c}, \quad \hat{\rho}_{l,\infty} = \frac{1}{V_l}, \tag{17}$$

where the terms of type V_j refer to the volumes involved in the interaction and $\Gamma_\nu V_s$ is the total volume of polymer per unit area.

Introducing the expressions for $\hat{\rho}$ in Eqs. (5) and (7), and carrying out the integrals in each region for the case of similar polymer layers $\hat{\rho}_k = \hat{\rho}_l$, we obtained the following expressions for the free energies of mixing:

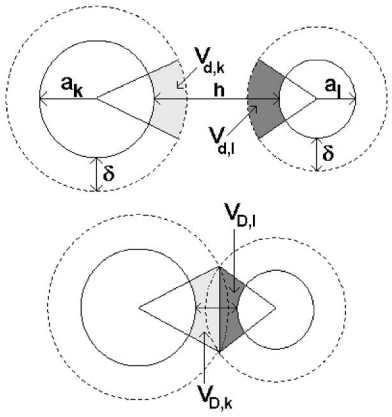

FIG. 5. Model for the calculation of the denting potential in EB model ($0 < h < 2\delta$).

$$\Delta G_M(h) = \frac{4k_BT}{3V_1}\bar{\phi}_{2,k}\bar{\phi}_{2,l}\left(\frac{1}{2} - \chi\right)\left(\delta - \frac{h}{2}\right)^2\left(\frac{3(a+b)}{2} + 2\delta + \frac{h}{2} - \frac{3(a-b)^2}{2(h+a+b)}\right), \quad \delta < h < 2\delta, \tag{18}$$

and

$$\Delta G_M(h) = \frac{k_BT}{V_1}\left(\frac{1}{2} - \chi\right) \times \left[(\bar{\phi}_{2,k})^2\left(\frac{V_k^2}{V_c} - V_k\right) + (\bar{\phi}_{2,l})^2\left(\frac{V_l^2}{V_c} - V_l\right) + 2\bar{\phi}_{2,k}\bar{\phi}_{2,l}\left(\frac{V_k V_l}{V_c}\right)\right], \quad 0 < h < \delta, \tag{19}$$

where

$$V_k = \frac{\pi\delta(20\delta^2 b - 6\delta h^2 + 8\delta^2 h - 12ah^2 + 8\delta^2 a + 3\delta^3 - 24bha + 12\delta ha - 12\delta hb + 36\delta ab)}{12(h+a+b)}, \tag{20}$$

$$V_l = \frac{\pi\delta(12\delta hb - 24ahb - 12bh^2 - 12\delta ha + 8\delta^2 h + 8b\delta^2 - 6\delta h^2 + 36b\delta a + 3\delta^3 + 2a\delta^2)}{12(h+a+b)}, \tag{21}$$

$$V_c = \frac{\pi(12\delta^3 a + 24\delta^2 ab + 6\delta^4 + 12\delta^3 b - 4h^3 a - 12h^2 ab - 4h^3 b - h^4)}{12(h+a+b)}. \tag{22}$$

In the above equations $a = a_k$ and $b = a_l$. For particles of equal size ($a = b$) these equations are considerably simplified, yielding

$$\Delta G_M(h) = \frac{4\pi k_BT}{3V_1}(\bar{\phi}_2)^2\left(\frac{1}{2} - \chi\right)\left(\delta - \frac{h}{2}\right)^2\left(3a + 2\delta + \frac{h}{2}\right), \quad \delta < h < 2\delta, \tag{23}$$

$$\Delta G_M(h) = \frac{2k_BT}{V_1}(\bar{\phi}_2)^2\left(\frac{1}{2} - \chi\right)\left(\frac{2V_a^2}{V_c} - V_a\right), \quad 0 < h < \delta, \tag{24}$$

where

$$V_a = \frac{\pi\delta(-24a^2h + 36\delta a^2 - 12a_k h^2 + 28\delta^2 a - 6h^2\delta + 3\delta^3 + 8h\delta^2)}{12(2a+h)}, \tag{25}$$

$$V_c = \frac{\pi(24a^2\delta^2 - 12a^2h^2 + 24\delta^3 a - 8ah^3 + 6\delta^4 - h^4)}{12(2a+h)}. \tag{26}$$

Notice that Eq. (23) reduces to the one obtained by Vincent *et al.* using the Derjaguin approximation when $\delta, h \ll a$. The same simplified equation was also obtained by Otewill and Walker [8] using a different treatment. However, these two researchers did not consider the appropriate expression for region $0 < h < \delta$, where considerable compression of the polymer layer occurs.

Figure 4 shows a comparison between the results obtained with the original Vincent model and the EV model for several particle radii. As previously explained, the difference between these two models is basically the use of the Derjaguin approximation. It is observed that this approximation works fine at relatively long distances of approach. The classification of the values of h as long, intermediate, and short used in this discussion depends on the relative magnitude of h with respect to the width of the stabilizing surfactant layer (where the steric interaction begins). As Fig. 4 shows, the Derjaguin approximation also works reasonably well at intermediate separations if the radius of the particles is sufficiently larger than the width of the polymer length ($\delta = 14.7$ nm in Fig. 4). This second observation is not surprising, since the mentioned condition is a typical requirement of the Derjaguin formalism: $\delta, h \ll a_0$. However, two major deviations are also evident from Fig. 4: (a) at very short distances of separation there is a significant overestimation of the repulsive potential in all cases; (b) for particles smaller than 100 nm, there is also an underestimation of the potential in the intermediate range of approach.

According to Eq. (23) which is valid when $\delta < h < 2\delta$, the steric potential is directly proportional to the volume of overlap. In the case of the Derjaguin approximation, the potential is also proportional to a volume, but the latter is just an approximation to the volume of overlap. As can be seen, the dependence of Eq. (24) ($0 < h < \delta$) on the volume of overlap is complex. The elastic contribution of the compressed chains is significant, and the spatial distribution of the polymer chains is more critical. In this region, the Derjaguin approximation fails even if $\delta, h \ll a_0$. This is more noticeable as the radius of the particles increases. These deviations of the Derjaguin approximation are due to its application to a repulsive force which depends on the volume of overlap. It is clear that, if the polymer molecules are grafted on a planar or a spherical surface, the distribution of monomer at a distance h from the surface of the body is different in each case. As a consequence, the polymer density is also distinct in the region of overlap. This deviation is more significant, if the volume of overlap is not calculated exactly.

IV. THE EB MODEL

Bagchi [2] carried out the direct calculation of the free energy of interaction between two identical spherical particles covered by polymer. For this purpose he evaluated the volume of overlap without the use of the Derjaguin approximation. He assumed a constant distribution of polymer around each particle, and used the expression of Flory and Huggins in order to compute the free energy of mixing.

Bagchi supposed the existence of two different interaction mechanisms, which may operate depending on the density of polymer molecules around each particle. At low polymer

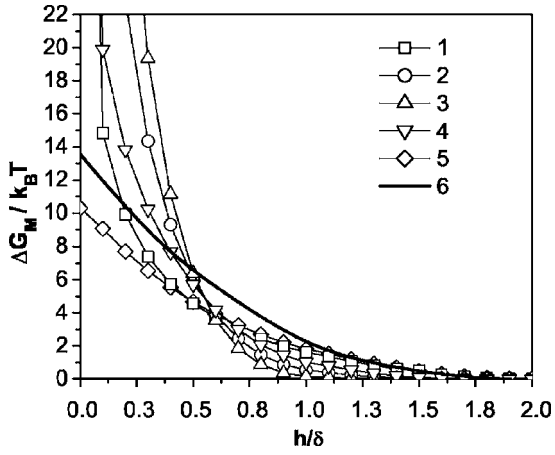

FIG. 6. Vincent model for different distributions of polymer segments around two spherical particles: 1=constant, 2=linear, 3=pseudohomopolymer, 4=pseudotails. EV model (curve 5) and DL experiment (curve 6). $a_k = a_l = 100$ nm, $\delta = 14.7$ nm.

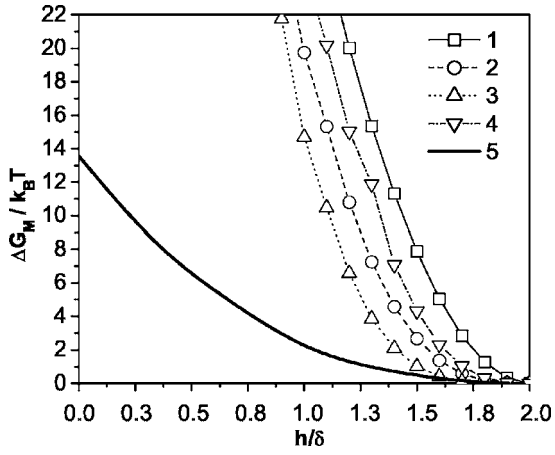

FIG. 7. Mixing contribution to the EB model for different distributions of polymer segments in the layers around particles: 1=constant, 2=linear, 3=pseudohomopolymer, 4=pseudotails, and DL experiment (curve 5). $a_k = a_l = 100$ nm, $\delta = 14.7$ nm.

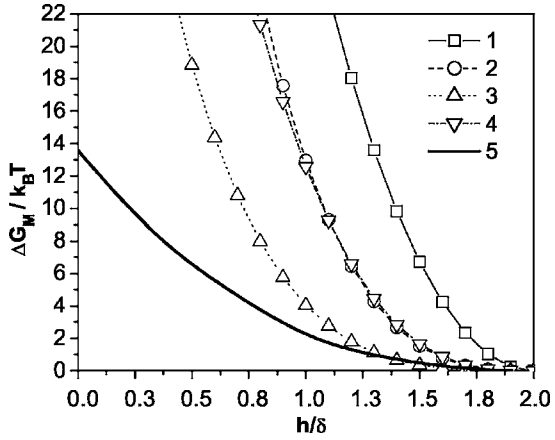

FIG. 8. Denting contribution to the EB model for different distributions of polymer segments in the layers around particles: 1 =constant, 2=linear, 3=pseudohomopolymer, 4=pseudotails, and DL experiment (curve 5). $a_k=a_l=100$ nm, $\delta=14.7$ nm.

coverage, Bagchi supposed a "mixing" mechanism: the polymer molecules coming from each particle adjust themselves to the volume of the overlap region displacing a given amount of solvent molecules toward the bulk. This mechanism is similar to the one previously described in the Introduction (Fig. 2). The second mechanism, formerly referred to as "denting," takes place at high polymer coverage. In this case the polymer molecules are "spontaneously" compressed and do not overlap. In this case the particle surfaces approach without the overlap of their polymer layers. The free energy of the system increases as each polymer layer is forced to occupy a smaller volume due its the interaction with the neighbor surface (see Fig. 5).

The free energy of interaction for each mechanism described above can be calculated using:

$$\Delta G_Z = (\Delta G_Z)^F - 2(\Delta G_Z)^I. \tag{27}$$

In Eq. (27), superscripts I and F stand for the initial and final states of the system, before and after the steric interaction occurs. The subscript $Z=M$ or D stands for the mechanisms of mixing (M) and denting (D). The free energy of interaction for either process $(\Delta G_Z)^X$ is given by the expression of Flory and Huggins:

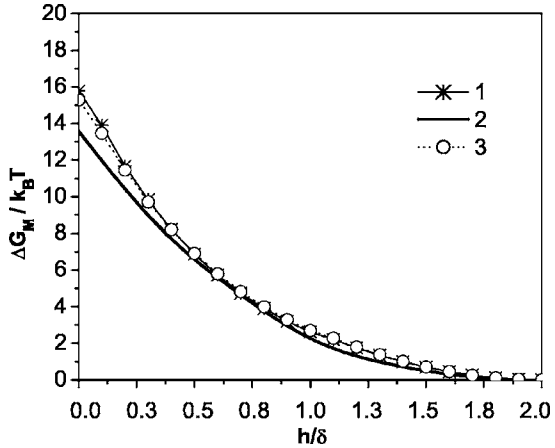

FIG. 9. (1) EB model predictions employing Eq. (41); (2) EV model predictions for $\bar{\phi}_2=0.0340$; (3) DL experiment. $a_k=a_l=100$ nm, $\delta=14.7$ nm.

TABLE I. Expressions for the calculation of $m_{2,j}^X$ and $m_{1,j}^X$ (mixing mechanism).

	Zone $\delta<h<2\delta$	
Initial	$m_{2,j}$	$V_j/\bar{V}_2$
	$m_{1,j}$	$\dfrac{(V_j-m_{2,j}^I\bar{V}_2)}{\bar{V}_1}$
Final	m_2	$m_{2,k}^I+m_{2,l}^I$
	m_1	$m_{1,k}^I+m_{1,l}^I-nm_2^F$
	Zone $0<h<\delta$	
Initial	$m_{2,j}$	$V_j/\bar{V}_2$
	$m_{1,j}$	$\dfrac{(V_j-m_{2,j}^I\bar{V}_2)}{\bar{V}_1}$
Final	m_2	$m_{2,k}^I+m_{2,l}^I$
	m_1	$m_{1,k}^I+m_{1,l}^I-nm_2^F-\bar{m}_1$
		$\bar{m}_1=\dfrac{V_e+V_f-\bar{m}_2\bar{V}_2}{\bar{V}_1}$
		$\bar{m}_2=\dfrac{V_f}{\bar{V}_2}+\dfrac{V_e}{\bar{V}_2}$

TABLE II. Equation for the calculation of $m_{2,j}^X$ and $m_{1,j}^X$ [denting mechanism $(0<h<2\delta)$].

Initial	$m_{2,j}$	$V_{d,j}/\bar{V}_2$
	$m_{1,j}$	$\dfrac{V_{d,j}-m_{2,j}^I\bar{V}_2}{\bar{V}_1}$
Final	m_2	$m_{2,k}^I+m_{2,l}^I$
	m_1	$m_{1,k}^I+m_{1,l}^I-\tilde{m}_{1,k}-\tilde{m}_{1,l}$
		$\tilde{m}_{1,j}=V_{D,j}\left(\dfrac{1-\bar{\phi}_{2,j}}{\bar{V}_1}\right)$

$$(\Delta G_Z)^X = N_a k_B T(m_1^X \ln \phi_1^X + m_2^X \ln \phi_2^X + \chi m_1^X \phi_2^X) \quad (28)$$

where the subscripts $X=I$ or F and $Z=M$ or D depending on the state of the system and the stabilization mechanism. N_a is Avogradro's number, and m_1^X, ϕ_1^X and m_2^X, ϕ_2^X are the number of moles and the volume fraction of solvent molecules (1) and polymer segments (2), in the volume of overlap before $(X=I)$ or after $(X=F)$ the interaction occurs (see Figs. 2 and 5). Variables ϕ_1^X and ϕ_2^X are given by

$$\phi_1^X = \left(\frac{m_1^X}{m_1^X + n m_2^X} \right), \quad (29a)$$

$$\phi_2^X = \left(\frac{n m_2^X}{m_1^X + n m_2^X} \right). \quad (29b)$$

Here, n is the coordination number of the lattice of water and polymer molecules used by Flory and Huggins in order to describe the polymer solution. It is equal to the ratio between the volume of one polymer molecule (V_2) and one solvent molecule (V_1): $n=V_2/V_1$.

In this way, ΔG_Z is determined once m_1 and m_2 are specified for the initial and final states. Bagchi related these variables directly to the volumes involved during the overlap. These volumes are obtained through geometric considerations and are expressed as a function of the distance of interaction between the particles, h, the extent of the polymer layer, δ, and the radius of the particles.

Figures 2 and 5 show the volumes involved during the overlap of the polymer layers for the mechanism of mixing and denting, respectively. Notice that the volumes can be defined over each sphere before and after the actual overlap occurs. For the mixing mechanism the volumes referred to change during the approach of the particles, while for the denting mechanism these volumes keep their geometric form through all approximation distances.

In order to extend the theory of Bagchi, we incorporated four different expressions for the distribution of polymer segments around each particle. These functions are similar to the ones previously proposed by Vincent *et al.* [1] for flat plates, except for the fact that we assumed a radial dependence of the polymer density instead of a linear one. Vincent *et al.* previously used a one-dimensional dependence in order to describe the interaction between two flat surfaces covered by polymer, prior to the application of the Derjaguin approximation. The distribution functions used in this work are

$$\phi_1(\varrho - a_j) = \bar{\phi}_{2,j}, \quad \text{constant}, \quad (30a)$$

$$\phi_2(\varrho - a_j) = 2\bar{\phi}_{2,j}\left(1 - \frac{\varrho - a_j}{\delta}\right), \quad \text{linear}, \quad (30b)$$

$$\phi_3(\varrho - a_j) = 3\bar{\phi}_{2,j}\left(1 - \frac{\varrho - a_j}{\delta}\right)^2, \quad \text{pseudohomopolymer}, \quad (30c)$$

$$\phi_4(\varrho - a_j) = \bar{\phi}_{2,j}\left(1 + \frac{2(\varrho - a_j)}{\delta} - \frac{3(\varrho - a_j)^2}{\delta^2}\right), \quad \text{pseudotail}, \quad (30d)$$

where $\varrho - a_j$ is the radial distance from the surface of the particles to the interaction zone. The radius of the particles is a_j, where $j=k$ or l as before. $\bar{\phi}_{2,j}$ is the volume fraction of polymer (subscript 2) around sphere j.

Each of the functions above is used to compute the quantities of polymer and solvent required for the evaluation of the steric interaction according to Bagchi. For the case of two polymer layers k and l surrounding spheres of radius a_k and a_l, Eq. (27) now becomes

$$\Delta G_Z = (\Delta G_{Z,kl})^F - (\Delta G_{Z,k} + \Delta G_{Z,l})^I \quad (31)$$

where the subscript kl denotes the overlap of the polymer layers k and l.

The terms appearing in Eq. (31) can be calculated following the procedure outlined by Bagchi [2] once $m_{1,j}^X$ and $m_{2,j}^X$ are specified (see the Appendix).

The fundamental difference of our procedure with the original method of Bagchi is that we use here functions of polymer density instead of constant polymer distributions. For this reason, the initial (I) amount of polymer contained in a volume V_j (Figs. 2 and 5) that will be present in the overlap region at distance of approach h, must be computed from function $\phi_i(\varrho - a_j)$. This quantity $[(m_{2,j}^i)^I]$ is given by

$$(m_{2,j}^i)^I = \frac{\int_{V_j} \phi_i(\varrho - a_j) dV}{\bar{V}_2} = \frac{V_j^i}{\bar{V}_2}, \quad (32)$$

where $\bar{V}_2$ is the molar volume of polymer, and index i specifies the type of distribution function used. When $i=1$ [constant distribution of polymer Eq. (30a)] and $a_k=a_j$, the expressions of Bagchi are recovered.

The integration over the volume of overlap suggested in Eq. (32) is analogous to that of the EV model and depends on the mechanism of stabilization (mixing or denting). When the distribution function is used, we found that the overlap occurs in an *effective volume* that depends on the mathematical form of the distribution function:

$$V_j^{i\neq 1} = \int_{V_j} \phi_{i\neq 1}(\varrho - a) dV = \bar{\phi}_2 \int_{V_j} f_{n\neq 1}(\varrho - a) dV = \bar{\phi}_2 v_{\text{eff}}. \quad (33)$$

Thus, the interactions are not obtained from the geometrical volume defined by the overlap of polymer layers such as is the case in a constant-density distribution where

$$V_j^1 = \int_{V_j} \phi_1(\varrho - a) dV = \int_{V_j} \bar{\phi}_2 dV = \bar{\phi}_2 \int_{V_j} dV = \bar{\phi}_2 v_{\text{geometric}}. \quad (34)$$

The volumes involved in the expressions $(m_{2,j}^i)^X$ and $(m_{1,j}^i)^X$ for the mixing mechanism in the region $\delta < h < 2\delta$ can be calculated using Eq. (35):

TABLE III. V_k^i for the calculation of the amount of polymer and solvent [mixing mechanism ($\delta<h<2\delta$)]. In the equations below $a=a_k$ and $b=a_l$. To obtain the volumes V_l^i interchange subscripts k and l and the radii a and b.

ϕ_i	V_k^i
ϕ_1	$\frac{\pi\bar{\phi}_{2,k}}{12}\frac{(h-2\delta)^2(h^2+4ha+4hb+4h\delta+12ab+4b\delta+4a\delta)}{(h+a+b)}$
ϕ_2	$\frac{\pi\bar{\phi}_{2,k}}{30}\frac{(2\delta-h)^3(2h^2-2\delta^2+10b\delta+7\delta h+20ab+5hb+10ah)}{\delta(h+a+b)}$
ϕ_3	$\frac{\pi\bar{\phi}_{2,k}}{20}\frac{(2\delta-h)^4(h^2-2\delta^2+4\delta h-2a\delta+6b\delta+6ha+10ab+2hb)}{\delta^2(h+a+b)}$
ϕ_4	$\frac{\pi\bar{\phi}_{2,k}}{60}\frac{(2\delta-h)^3(4\delta^3+12\delta^2a+4\delta^2b-2\delta^2h+14\delta h^2-2\delta ha+26\delta hb+20\delta ab+3h^3+18h^2a+6bh^2+30hab)}{\delta^2(h+a+b)}$

$$V_k^i=\int_0^{2\pi}\int_0^{\cos^{-1}(p_k/R_k)}\int_{H\cos(\varphi)-[R_l^2+H^2\cos^2(\varphi)-H^2]^{1/2}}^{R_k}\phi_i(\rho-a_k)\times\varrho^2\sin(\varphi)d\varrho\,d\varphi\,d\theta. \tag{35}$$

For the calculation of $(m_{2,l}^i)^I$, we can obtain volume V_l^i by interchanging the subscripts k and l in the last equation. Notice that in this interaction region the volumes of overlap identified before and after the actual superposition occurs have the same geometrical form, Fig. 2(a).

In the region $0<h<\delta$ [Fig. 2(b)], the expressions used for the calculation of these volumes are

$$V_k^i=\int_0^{2\pi}\int_0^{\cos^{-1}(p_k/R_k)}\int_{H\cos(\varphi)-[R_l^2+H^2\cos^2(\varphi)-H^2]^{1/2}}^{R_k}\phi_i(\rho-a_k)\varrho^2\sin(\varphi)d\varrho\,d\varphi\,d\theta-\int_0^{2\pi}\int_0^{\cos^{-1}(q_k/a_k)}\int_{H\cos(\varphi)-[R_l^2+H^2\cos^2(\varphi)-H^2]^{1/2}}^{a_k}\phi_i(\rho-a_k)\varrho^2\sin(\varphi)d\varrho\,d\varphi\,d\theta, \tag{36}$$

$$V_f^i=\int_0^{2\pi}\int_0^{\cos^{-1}(Q_k/R_k)}\int_{H\cos(\varphi)-[a_l^2+H^2\cos^2(\varphi)-H^2]^{1/2}}^{R_k}\phi_i(\rho-a_k)\varrho^2\sin(\varphi)d\varrho\,d\varphi\,d\theta, \tag{37}$$

For the denting interaction the following equations are obtained for the volumes $V_{d,k}^i$ and $V_{D,k}^i$ (Fig. 5):

$$V_{d,k}^i=\int_0^{2\pi}\int_0^{\cos^{-1}(p_k/R_k)}\int_{a_k}^{R_k}\phi_i(\rho-a_k)\varrho^2\sin(\varphi)d\varrho\,d\varphi\,d\theta, \tag{38}$$

$$V_{D,k}^i=\int_0^{2\pi}\int_0^{\cos^{-1}(p_k/R_k)}\int_P^{R_k}\phi_i(\rho-a_k)\varrho^2\sin(\varphi)d\varrho\,d\varphi\,d\theta, \tag{39}$$

where $P=p_k\sec(\varphi)$.

The volumes V_l^i, V_e^i, $V_{d,l}^i$, and $V_{D,l}^i$ and the distances p_l, q_l and Q_l are obtained interchanging subscripts k and l in Eqs. (35)–(39) and (11a)–(11c), respectively. The explicit formulas calculated in this work for the volumes appearing in Eqs. (35)–(39) are given in the Appendix (Tables III–V).

This model (EB model) has the advantage that the geometry is spherical right from the start. Unlike EV model, the expressions obtained are analytic for each polymer distribution function corresponding to Eqs. (30a)–(30d). However, the most important disadvantage is that it does not follow the formalism of Meier, which is widely accepted to treat the mixing term of the steric potential. Instead, Bagchi applies directly the Flory-Huggins expression

$$\Delta G_M=k_BT(n_1\ln\bar{\phi}_1+n_2\ln\bar{\phi}_2+\chi n_1\bar{\phi}_2). \tag{40}$$

Notice that the second term in the expression above is equal to zero for grafted polymer layers, since it corresponds to the configurational entropy of the center of mass of the polymer molecules [30]. As a consequence, the potentials calculated are likely to overestimate the true interaction potential. A possible improvement of this formalism can be achieved simply disregarding the second term in Eq. (40). This gives an expression for the energy of mixing similar to the one of Flory and Krigbaum:

$$\Delta G_M=k_BT(n_1\ln\bar{\phi}_1+\chi n_1\bar{\phi}_2). \tag{41}$$

TABLE IV. V_k^i for the calculation of the amount of polymer and solvent [mixing mechanism $(0<h<\delta)$]. In the equations below $a=a_k$ and $b=a_l$. To obtain the volumes V_l^i interchange the subscripts k and l and the radii a and b.

V_k^1	$\frac{\pi\delta\bar{\phi}_{2,k}}{12}\frac{(36a\delta b+8\delta^2 h+12\delta ha-12\delta hb-6\delta h^2-24hab-12h^2a+20\delta^2 b+8a\delta^2+3\delta^3)}{(h+a+b)}$
V_f^1	$\frac{\pi\bar{\phi}_{2,k}}{12}\frac{(h-\delta)^2(h^2+4hb+4ha+2h\delta+12ab-3\delta^2-4a\delta+8b\delta)}{(h+a+b)}$
V_k^2	$\frac{\pi\delta\bar{\phi}_{2,k}}{30}\frac{(7\delta^3+25a\delta^2-30h^2a+20ha\delta-10h^2\delta+80ab\delta-20hb\delta-60hab+30b\delta^2+10h\delta^2)}{(h+a+b)}$
V_f^2	$\frac{\pi\bar{\phi}_{2,k}}{30}\frac{(h-\delta)^3(5a\delta-2h^2-5ha-10hb-h\delta-20ab-10b\delta+3\delta^2)}{\delta(h+a+b)}$
V_k^3	$\frac{\pi\delta\bar{\phi}_{2,k}}{20}\frac{(4h\delta^2+14b\delta^2+18a\delta^2+10ha\delta-10hb\delta-40hab+50ab\delta-20h^2a+4\delta^3-5h^2\delta)}{(h+a+b)}$
V_f^3	$\frac{\pi\bar{\phi}_{2,k}}{20}\frac{(h-\delta)^4(h^2+6hb+2ha+10ab-2a\delta+4b\delta-\delta^2)}{\delta^2(h+a+b)}$
V_k^4	$\frac{\pi\delta\bar{\phi}_{2,k}}{60}\frac{(16\delta^3+46a\delta^2-50hb\delta-120hab+50ha\delta+170ab\delta+28h\delta^2+78b\delta^2-60h^2a-25h^2\delta)}{(h+a+b)}$
V_f^4	$\frac{\pi\bar{\phi}_{2,k}}{60}\frac{(h-\delta)^3(-3h^3-6h^2a-18bh^2-5\delta h^2-8\delta ha-34\delta hb-30hab-\delta^2h-14a\delta^2-50\delta ab-28\delta^2b+9\delta^3)}{\delta^2(h+a+b)}$

V. COMPUTATIONAL DETAILS

Using a Langmuir trough, Doroszkowski and Lambourne (DL) measured the variation of the surface pressure (Π) as a function of the total interfacial area (A_t) for spheres of polyacrylonitrile suspended at the toluene/water interface. The particles were stabilized sterically by polystyrene tails and the work of compression calculated from the product ΠA_t. The determination of the potential was possible assuming that the number of contacts of one sphere at the interface was equal to six as in an hexagonal close-packed arrangement. The resulting experimental curve is shown in Fig. 6 (curve 5).

In order to parametrize the theoretical expressions for the EV and EB models, the following experimental values were used [11]: $a_k=a_l=100$ nm, $V_2=0.91$ cm^3/g, $V_1=107$ cm^3/mol, $M_W=6000$ g/mol, $\Gamma=5.2\times10^{-8}$ g/cm^2, $\delta=14.7$ nm, and $\chi=0.468$.

The average volume fraction of polymer around each particle was calculated following Eq. (42):

$$\bar{\phi}_{2,j}=\frac{3a_j^2\Gamma V_2}{\delta^3+3a_j\delta^2+3\delta a_j^2}. \tag{42}$$

In this equation the total amount of polymer is obtained by multiplying the surface excess of the polymer molecules by the area of the drops. The volume fraction can be calculated using the molar volume of the polymers ($\overline{V_2}$) and the volume of the polymer shell around each particle [denominator of Eq. (42) divided by 3]. The volume fraction obtained was $\phi_2=0.0279$. The average molar concentration of polymer around each particle was equal to $c=\bar{\phi}_2/\overline{V_2}$, and the "coordination number of the lattice" was equal to $n=\overline{V_2}/\overline{V_1}$.

TABLE V. $V^i_{d,k}$ and $V^i_{D,k}$ for the calculation of the amount of polymer and solvent in the denting mechanism ($0<h<2\delta$). In the equations below $a=a_k$ and $b=a_l$. To obtain volumes $V^i_{d,l}$ and $V^i_{D,l}$ interchange subscripts k and l and radii a and b.

$V^1_{d,k}$

$$\frac{\pi\delta\bar{\phi}_{2,k}}{3}\frac{(3a^2+3\delta a+\delta^2)(h+2\delta)(h+2b)}{(h+a+b)(a+\delta)}$$

$V^1_{D,k}$

$$\frac{\pi\bar{\phi}_{2,k}}{24}\frac{(h-2\delta)^2(h^2+2hb+6ha+4h\delta+6ab+6a\delta+2b\delta+6a^2)(h+2b)^2}{(h+a+b)^3}$$

$V^2_{d,k}$

$$\frac{\pi\delta\bar{\phi}_{2,k}}{6}\frac{(6a^2+4\delta a+\delta^2)(h+2\delta)(h+2b)}{(h+a+b)(a+\delta)}$$

$V^2_{D,k}$

$$\frac{\pi\bar{\phi}_{2,k}}{48}\frac{(h-2\delta)^3(h+2b)^3(h-2a)(2a+2b+h+2\delta)}{\delta(h+a+b)^4}$$

$V^3_{d,k}$

$$\frac{\pi\delta\bar{\phi}_{2,k}}{10}\frac{(10a^2+5\delta a+\delta^2)(h+2\delta)(h+2b)}{(h+a+b)(a+\delta)}$$

$V^3_{D,k}$

$$\frac{\pi\bar{\phi}_{2,k}}{320}\frac{(h-2\delta)^4(h+2b)^4)(6hb+10ab-2b\delta+3h^2+10ha+4\delta h+10a^2+10a\delta)}{\delta^2(h+a+b)^5}$$

$V^4_{d,k}$

$$\frac{\pi\delta\bar{\phi}_{2,k}}{30}\frac{(30a^2+25a\delta+7\delta^2)(h+2\delta)(h+2b)}{(h+a+b)(a+\delta)}$$

$V^4_{D,k}$

$$\frac{\pi\bar{\phi}_{2,k}(h-2\delta)^3(h+2b)^3(4hb^2\delta-36h^2b^2-60hb^2a-40b^2a\delta-24b^2\delta^2-36h^3b-66h^2b\delta-90h^2ab-44hb\delta^2-280hab\delta-60ha^2b-200b\delta a^2)}{960\delta^2(h+a+b)^5}$$

$$+\frac{\pi\bar{\phi}_{2,k}(h-2\delta)^3(h+2b)^3(-40ab\delta^2-9h^4-30h^3a-34\delta h^3-56h^2\delta^2-30h^2a^2-170h^2a\delta-180ha\delta^2-260ha^2\delta-160\delta^2a^2-160\delta a^3)}{960\delta^2(h+a+b)^5}$$

VI. COMPARISON BETWEEN EV AND EB MODELS

Figure 6 shows the prediction of the Vincent model for constant (curve 1), linear (curve 2), pseudohomopolymer (curve 3), and pseudotail (curve 4) polymer distributions. The formulas used for the calculation of these plots are the ones previously reported by Vincent *et al.* [1]. They were calculated from Eq. (2) using different theoretical polymer distributions [constant (C), pseudohomopolymer (PH), linear (L), and pseudotail (PT)] along with the Derjaguin approximation. As can be observed, all the potentials lie fairly close to the experimental measurement of Doroszkowski and Lambourne. However, all of them underestimate the experimental measurement at intermediate distances of approach, and drastically overestimate it at very close separations. Out of

the four polymer distributions tested, the prediction of the constant polymer distribution (C) lies closer to the experimental curve at these two distances. Instead, PH, L, and PT fall closer to the experimental measurements at intermediate separations. Figure 6 also shows the prediction of the EV model proposed for a constant polymer distribution. The EV curve has a similar shape to the one of the DL potential: it follows the qualitative variation of the DL (curve 6 in Fig. 6) presenting a finite limit for $h=0$ ($V_S=25k_BT$).

On the other hand, the predictions of the extended Bagchi model are substantially displaced to longer distances of approach for all polymer distributions proven (Figs. 7 and 8). In this case, the PH distribution falls closer to the DL curve, while the constant polymer distribution C is the one that lies farther away.

The nature of the deviation of the EB model with respect to DL can be understood by looking at Eqs. (40) and (41). The expression of mixing calculated from Flory-Huggins theory has an additional term as compared to the one from Flory-Krigbaum theory. Elimination of that additional term is equivalent to using Flory-Krigbaum theory within the EB formalism. The result from this procedure is shown in Fig. 9. This prediction of EB for the constant polymer distribution lies very close to the DL measurement, and follows the shape of the experimental curve along the whole range of the potential.

In the case of EV, the nature of the deviation is very different. Figure 9 also shows the prediction of the EV model for an adjusted value of the average polymer distribution around each particle. Using $\bar{\phi}_2=0.0340$ instead of 0.0279 yields curve 2 in Fig. 9. The curve basically coincides with the prediction of the EB model when Flory-Krigbaum formalism is used.

VII. CONCLUSION

In this paper possible extensions of the work of Vincent (EV) and Bagchi (EB) were presented. Explicit analytic expressions for the mixing contribution of the steric potential are put forward for the case of two spheres of different radii. These expressions avoid the use of Derjaguin approximation.

The use of experimental parameters in the EV model gives a fair prediction of the DL curve. However, an adjustment of the volume fraction of polymer is required in order to reproduce the experimental results. This is an indication that a different polymer distribution might be able to reproduce the experimental curve without further adjustment.

On the other hand, the EB model is only able to approach the experimental measurements of DL if the formalism of Flory-Krigbaum is used to calculate the mixing term. In this case, a constant polymer distribution produces a prediction of a similar quality to that of the EV model. Otherwise, the EV model works considerably better than the EB one.

APPENDIX: CALCULATION OF PARAMETERS FOR THE EB MODEL

The calculation of ΔG_Z employing Eq. (31) requires the specification of each term included in Eq. (28). These are determined once the amounts of polymer (m_2^X) and solvent (m_1^X) are given for the overlap region, before and after the actual overlap of the polymer layers occurs (Figs. 2 and 5). Those quantities are calculated in a different manner depending on the mechanism of stabilization (mixing or denting). In addition, in the case of mixing it must be taken into account that the volume of overlap changes when the separation distance goes from $\delta<h<2\delta$ to $0<h<\delta$.

The equations that allow the calculation of (m_2^X) and (m_1^X) are summarized in Tables I and II for the different cases outlined above. These equations were written following the original work of Bagchi [2]. The difference between our equations and the original ones is that the volume of overlap is calculated considering several distribution functions other than the constant one. In Tables I and II, the superindex i has been omitted for simplicity. However, this index identifies the distribution function. Thus, it should be kept in mind that there exist a similar set of equations as the ones given in Tables I and II for each distribution function of polymer segments.

The quantity m_2^I (I=initial) is the amount of polymer that there is in the volume over which the overlap will occur in each sphere ($j=k$ or l). This is true for the cases of mixing and denting. The variable m_1^I stands for the amount of solvent that can be accommodated in the same region, once the polymer has been distributed. The variable m_2^F (F=final) is equal to the sum of the initial amount of polymer contained in the overlap region of each sphere, before the overlap occurs. The procedure for the calculation of m_1^F is similar to that of m_1^I, the difference being that the volumes that must be taken into account are different. As a consequence, the equations of Tables I and II for these two cases are distinct.

The volumes that appear in the equations of Tables I and II are given by Eqs. (35)–(39) in integral form, and their explicit analytical expressions are given in Tables III–V for each distribution function employed in this work. When the constant distribution function is used ($i=1$) the calculation of ΔG_Z is equal to the one originally published by Bagchi [2], except for the fact that the present equations were developed for particles of different radii.

[1] B. Vincent, J. Edwards, S. Emmett, and A. Jones, Colloids Surf. **18**, 261 (1986).
[2] P. Bagchi, J. Colloid Interface Sci. **47**, 86 (1974).
[3] E. L. Mackor, J. Colloid Sci. **6**, 492 (1951).
[4] R. H. Otewill, J. Colloid Interface Sci. **58**, 357 (1977).
[5] D. J. Meier, J. Phys. Chem. **71**, 1861 (1967).
[6] F. T. Hesselink, J. Phys. Chem. **75**, 2094 (1971).
[7] A. K. Dolan and S. F. Edwards, Proc. R. Soc. London, Ser. A

343, 427 (1975).
[8] R. H. Otewill and T. Walker, Kolloid Z. Z. Polym. **227**, 108 (1968).
[9] A. Doroszkowski and R. Lambourne, J. Colloid Interface Sci. **41**, 97 (1973).
[10] R. Evans and D. H. Napper, Kolloid Z. Z. Polym. **251**, 329 (1973).
[11] J. B. Smitham, R. Evans, and D. H. Napper, J. Chem. Soc., Faraday Trans. 1 **71**, 285 (1975).
[12] B. V. Derjaguin, N. V. Churaev, and V. M. Muller, *Surfaces Forces* (Plenum Publishing, New York, 1994).
[13] I. Szleifer, Curr. Opin. Colloid Interface Sci. **1**, 416 (1996).
[14] J. M. Scheutjens and G. J. Fleer, Adv. Colloid Interface Sci. **16**, 361 (1982).
[15] P. G. de Gennes, Adv. Colloid Interface Sci. **27**, 189 (1987).
[16] H. J. Tauton, C. Toprakcioglu, and J. K. Ll. Fetters, Macromolecules **23**, 571 (1990).
[17] M. B. Einarson and J. C. Berg, J. Colloid Interface Sci. **155**, 165 (1993).
[18] J. L. Ortega-Vinuesa, A. Martín-Rodríguez, and R. Hidalgo-Alvarez, J. Colloid Interface Sci. **184**, 259 (1996).
[19] J. A. Lewis, J. Am. Ceram. Soc. **83**, 2341 (2000).
[20] S. M. Oversteegen and H. N. W. Lekkerkerker, Physica A **341**, 23 (2004).
[21] A. Doroszkowski and R. Lambourne, J. Polym. Sci., Part C: Polym. Symp. **34**, 253 (1971).
[22] J. Klein and P. F. Luckham, Macromolecules **18**, 721 (1985).
[23] J. Israelachvili, M. Tirrell, and Y. A. J. Klein, Macromolecules **17**, 204 (1984).
[24] J. Klein and P. F. Luckham, Macromolecules **17**, 1041 (1984).
[25] A. Homola and A. A. Robertson, J. Colloid Interface Sci. **54**, 286 (1976).
[26] O. Mondain-Monval, A. Espert, P. Omarjee, F. Leal-Calderon, J. Philip, and J. Joanny, Phys. Rev. Lett. **80**, 1778 (1998).
[27] J. Bibette, F. Leal-Calderon, and P. Poulin, Rep. Prog. Phys. **62**, 969 (1999).
[28] P. J. Flory and W. R. Krigbaum, Macromolecules **18**, 1086 (1950).
[29] P. J. Flory, *Principles of Polymer Chemistry* (Interscience, New York, 1952).
[30] D. H. Napper, *Polymer Stabilization of Colloidal Dispersions* (Academic Press, London, 1983).